The guiding effect of artificially injected gas bubble on the underwater pulsed spark discharge and its electrical and acoustic parameters after breakdown

Xu Guo, Ying Sun[1], Chen-Lei Liu, Lin Jing, Yuan-Tao Zhang, Xiao-Long Wang
School of Electrical Engineering, Shandong University,
Jinan, Shandong Province, 250061, P. R. China
Igor Timoshkin
Department of Electronic and Electrical Engineering, University of Strathclyde,
Glasgow, G1 1XW, United Kingdom

Abstract

The presence of a low density area is beneficial to the facilitation of the underwater pulsed spark discharge, which can be achieved by artificially injecting gas bubble in between the inter-electrode gap. The generation of intensive acoustic waves by such gas-bubble-guided spark discharges makes them promising underwater acoustic sources in multiple practical applications. This paper is aimed at comprehensive investigation of the guiding effect of the injected bubble on the pre-breakdown process of underwater pulsed spark discharges and potential correlations between their subsequent electrical and acoustic parameters with the purpose of optimizing the acoustic emission. The breakdown probability and the pre-breakdown delay were used to evaluate the general facilitation effect brought by the injected bubble. Experimental and numerical works have been conducted and allow observation on the dynamics of the injected bubble under the influence of the applied voltage. Different guiding modes of the injected bubble for plasma streamers' propagation has been observed regarding its relative position. The characteristics of the electrical properties of gas-bubble-guided spark discharges, including the plasma resistance and the plasma energy density, were analyzed by relating them with the breakdown voltage. The dependency of the acoustic wave amplitude and the acoustic efficiency on these electrical parameters was verified which provides solid regulation principles for the optimization of the plasma-acoustic system for target practical applications.

***Index Terms*—**Underwater pulsed spark discharge, artificially injected gas bubble, bubble dynamics, plasma resistance, plasma energy density, acoustic parameters.

[1] ys2018@sdu.edu.cn

I. INTRODUCTION

Underwater pulsed spark discharge (UPSD) produces a serious of physical and chemical phenomena by applying high voltage impulse between electrodes in dielectric water, including light emission, cavity oscillation, active particles and especially the acoustic waves (AWs). The amplitude of these UPSD-generated AWs can be tailored from tens to thousands of MPa, by using appropriate discharge geometry and energization conditions [1]. Also, their bandwidth covers a large range of frequency from hundreds of Hz to tens of MHz [2]. Therefore, UPSD, as a promising underwater acoustic source, has been used widely in, for example, medical shock wave crushing, petroleum and gas extraction, rock crushing, waste water treatment, marine exploration and other fields [3-14].

The generation of the shock wave corresponds to the expansion of the plasma channel after breakdown and it decays to acoustic wave after propagation [15, 16]. In [17], it was shown that the magnitude of UPSD-generated AWs is highly related to the initial electrical power delivered into plasma during the first current oscillation cycle after breakdown. Thus, the peak pressure value of these AWs depends on the residual electrical energy stored in the capacitors at breakdown [18], and it is found to be proportional to the product of the storage capacitance, C, to the power of $1/3\beta$ and the breakdown voltage, V_{br}, to the power of $2/3\beta$, where the value of β is 1.13, as $P_{ac} \propto C^{\beta/3} V_{br}^{2\beta/3}$ [19]. However, the increase in the electrical energy does not always yield significant improvement in the magnitude of plasma-generated AWs, especially when the electrical energy has already researched a relatively high level [20], resulting in lower acoustic efficiency. The inter-electrode gap distance determines the maximal magnitude of achievable AWs [21]. In this case, the favorable breakdown scenario to generate intense AWs with relatively high energy conversion efficiency can be summarized as breakdown in long inter-electrode gap with short pre-breakdown delay by using voltage impulses with approximate (not with extremely large) amplitude.

Traditional untriggered UPSDs is characterized by free discharge propagation space between electrodes. The presence of pulsed voltage drives the charge injection on the electrode and the modified electric field initiates discharge streamers [22]. Then, these streamers propagate from high voltage (HV) electrode to the opposite one to finish breakdown and this propagation may take a few steps, depending on the voltage amplitude [23]. In the case of untriggered UPSDs, randomly-formed propagation pathway (plasma channel) between electrodes tends to cause longer pre-breakdown delay and thereby lower electrical energy stored at breakdown [24]. Therefore, untriggered UPSDs may not be preferable when considering to achieve the favorable breakdown scenario as mentioned above. Besides, unpredictable plasma channel tracks of such UPSDs conflict with the stable acoustic emission requirement from the point of view of practical applications [25].

An effective method to reduce the pre-breakdown delay for UPSDs in long gaps is injection of gas bubbles in between electrodes [26]. The introduction of low-density areas not only enhances the electric field due to the difference in the permittivity of dielectric water and gaseous bubbles, but also provides lower breakdown strength for easier discharge initiation [27, 28]. These features would potentially reduce the electrical loss before breakdown [29], especially for dielectric water with elevated electrical conductivity. As reported in [30], the discharge was initiated and propagated inside the gas bubble when it was in close contact with electrodes. Similar observation was made in [31]. In addition, the discharge was found to be confined within individual bubble and the upcoming development of discharge tended to cause the bubble blast when using voltage impulse with relatively large amplitude, for example 30 kV. In [32], it was found that the initial streamer normally formed on the pin electrode and the gas bubble acted as a bridge to guide the initial streamer to propagate to the opposite electrode when the gas bubble was present at a distance from the pin electrode. Also, the hydrodynamic behaviors of these injected gas bubbles will be influenced by the existence of the applied

This is a peer-reviewed, accepted author manuscript of the following research article:
Guo, X., Sun, Y., Liu, C-L., Jing, L., Zhang, Y-T., Wang, X-L., & Timoshkin, I. (2022). The guiding effect of artificially injected gas bubble on the underwater pulsed spark discharge and its electrical and acoustic parameters after breakdown. Physics of Plasmas, 29(11), [113504]. https://doi.org/10.1063/5.0122080

voltage impulse, which is mainly contributed to the electric stress performed at the water/gas interface [33, 34]. Therefore, the interaction between the injected gas bubble and the high voltage impulse is complex. The resultant guiding effect of such bubbles is crucial for understanding the breakdown mechanism of modified UPSDs, which has not been thoroughly investigated.

This paper focuses on the development of pre-breakdown stage of bubble-guided UPSDs and the correlations between their electrical and acoustic parameters after breakdown. Gas bubbles were injected between inter-electrode gap and time-resolved imaging diagnosis were adopted to investigate the dynamic behavior of these bubbles at the presence of HV impulses and their guiding effect during the discharge development stage. A two-dimensional numerical model was established combing the electric stress and the phase field method [35, 36] in order to explain deformation characteristics of bubbles under different charging voltages. Electrical parameters of the plasma channel after breakdown were obtained by using constant resistance model [37], including the breakdown voltage, the plasma resistance, the plasma energy and the plasma energy density. The functional dependency of acoustic amplitude and efficiency on these electrical parameters were also obtained and analyzed. These results will help to construct a comprehensive picture for the gas-bubble-guided plasma-acoustic system and to optimize its design for specific application by reasonably manipulating the discharge process.

II. EXPERIMENT SETUP

The experimental setup used in this paper is demonstrated in Fig. 1(a), including pulsed-power system, discharge electrodes with bubble injection system and diagnostic devices. The pulsed power system is composed of a HV DC power supply (EMPEAK HPS-60-120), storage capacitors (PLUSPARK) and a self-made spark switch. The storage capacitors were charged by the DC power supply and voltage impulse was generated by triggering the spark switch. The voltage amplitude varied from 20 kV to 35 kV and the capacitance of 400 nF was used in this paper. The rise time of the generated voltage impulse was less than 100 ns and the pulse width was approximately 400 μs.

The discharge electrodes established in this paper included two different sets, one set for free-bubble injection and the other set for fixed-bubble injection. The free-bubble electrodes set, composed of a conical HV electrode and a cylindrical ground electrode as shown in Fig. 1(b), was used to study the general breakdown performance of gas-bubble-guided UPSDs and their corresponding electrical and acoustic properties. By pumping air into the gas flow channel (embedded within the ground electrode) from the inlet port, installed at the side bottom of the ground electrode, free bubbles were able to be generated coming from the circular outlet port (with diameter of 1 mm) located at the central position on the top of the ground electrode. In this case, injected bubbles would move vertically from the ground electrode towards the upper HV electrode. The air flow rate was precisely controlled by using a gas mass flow controller (ALICAT MC-Series) during experiments to maintain the steady free-floating of bubbles between the electrodes. The fixed-bubble electrodes set was used to investigate the influence of the position and the size of gas bubble on its guiding effect on breakdown mechanism of UPSDs. These particular electrodes set, as shown in Fig. 1 (c), consisted of a pin HV electrode, the same cylindrical ground electrode as used in the free-bubble electrodes set (with the pump off), and a capillary tube with diameter of 1 mm. The gas bubble was generated and kept attached at the output end of the capillary tube by using a syringe to support air injection from the other end of the tube. Therefore, the position of the generated bubble would follow the adjustment of the capillary tube. These electrodes sets were placed in the middle of a water container (with the size of 1 m (length) * 0.7 m (width) *0.7 m (height)) to be powered to achieve UPSDs. Two quartz-glass observation windows were installed respectively on two sides of the water container for optical diagnosis. The dielectric liquid was local tap water with electrical conductivity of 800 μS/cm.

This is a peer-reviewed, accepted author manuscript of the following research article:
Guo, X., Sun, Y., Liu, C-L., Jing, L., Zhang, Y-T., Wang, X-L., & Timoshkin, I. (2022). The guiding effect of artificially injected gas bubble on the underwater pulsed spark discharge and its electrical and acoustic parameters after breakdown. Physics of Plasmas, 29(11), [113504]. https://doi.org/10.1063/5.0122080

The voltage and current waveform were measured by a high-voltage probe (NorthStar PNM-7, 1:1000) and a Rogowski coil (PEMCWT HF 600/B, calibration scale 0.05mV/A), respectively. Acoustic signals were collected using a hydrophone (Hangzhou Maihuang Technology Co, RSH-10, frequency range 20-120kHz, sensitivity -210dB, calibration scale 31.62 V/Mpa). These waveforms were recorded in an oscilloscope (Agilent Technologies, DSO1024A). Time-resolved images of the discharge channel were captured using the shadow method with a collimated LED light source (Dongguan Kemai Vision Technology Co, DCS2.0), a high-speed camera (FASTEC IMAGIN, HiSpec5 4G, max frame rate 112,138fps, resolution 128*2, pixel size 14*14 μm) and discharge gap in one straight line.

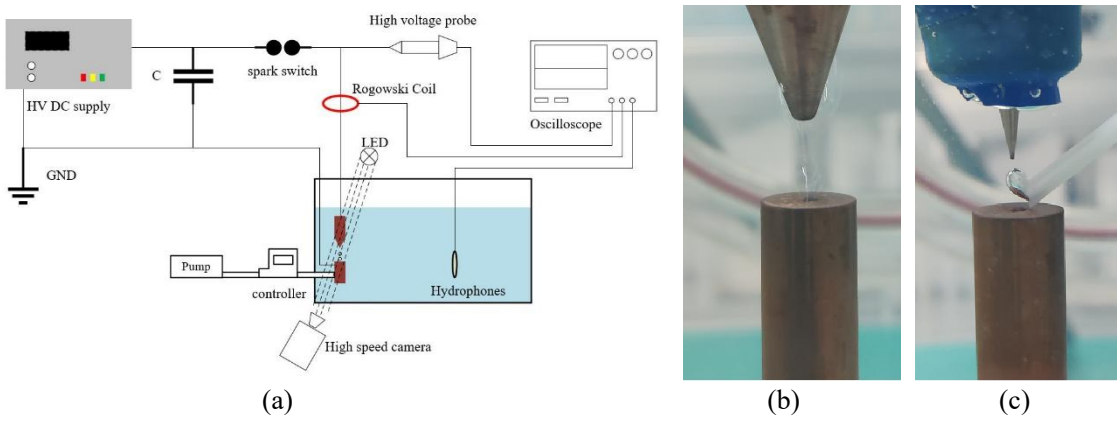

FIG. 1. Experimental setup. (a) schematic diagram of the platform, (b) the conical HV electrode and the ground electrode embedded with gas flow channel, (c) the pin-plate electrodes and the capillary tube used for fixed-bubble injection.

III. RESULTS AND DISSCUSSION

A. The role of injected bubble in pre-breakdown stage of UPSDs

The randomness in the development of plasma streamers in untriggered UPSDs cases will cause fluctuation in pre-breakdown delay, resulting in unstable repeated breakdown performance under same energization conditions. The introduction of the injected bubble not only enhance the intensity of local electric filed strength, also provides potential shortcuts for streamers to propagate. In another words, the guiding effect of the injected bubble on the streamers' development makes it possible to manipulate the breakdown process and to obtain desirable electrical and acoustic parameters.

1. General effect of injected bubble on breakdown probability and pre-breakdown delay

The analysis on the breakdown facilitation induced by the injected bubble was conducted by comparing the breakdown probabilities of untriggered and free-bubble-guided UPSDs in this section. For each combination of inter-electrode gap

This is a peer-reviewed, accepted author manuscript of the following research article:
Guo, X., Sun, Y., Liu, C-L., Jing, L., Zhang, Y-T., Wang, X-L., & Timoshkin, I. (2022). The guiding effect of artificially injected gas bubble on the underwater pulsed spark discharge and its electrical and acoustic parameters after breakdown. Physics of Plasmas, 29(11), [113504]. https://doi.org/10.1063/5.0122080

distance and charging voltage, at least 30 discharge shots were fired for either type of UPSDs to ensure the statistical accuracy. Then, the breakdown probability was defined as the ratio between the count number of successful breakdowns and the count number of total fired discharges.

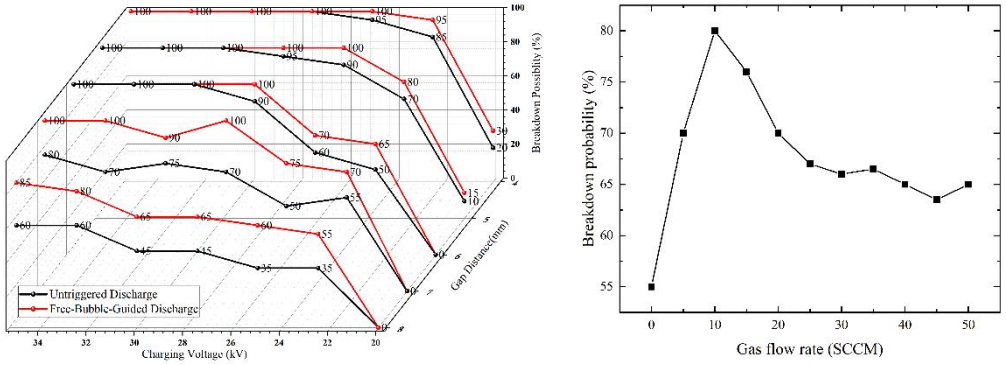

(a) (b)

FIG.2. (a) Breakdown probability of untriggered UPSDs and gas-bubble-guided UPSDs under different combinations of gap distance and charging voltage, (b) dependency of breakdown probability on gas flow rate obtained at 30 kV and 6 mm gap.

Fig. 2(a) demonstrates breakdown probability obtained for untriggered and free-bubble-guided UPSDs under different discharge conditions. It can be seen that the probabilities of successful breakdown for both untriggered and free-bubble-guided UPSDs are similar, regarding relatively short gap distances, for example, 4 and 5 mm. For longer gap distances, although the increase in charging voltage yields higher breakdown probabilities as larger voltage amplitude initiates stronger and faster streamers to electrically bridge the inter-electrode gap, the introduction of free bubbles still provides further increase, approximately 15% to 25%, in the value of breakdown probabilities as compared with untriggered UPSDs under same discharge conditions. Such improvement is more significant when considering to achieve breakdown in long inter-electrode gap by using voltage impulse with relatively lower amplitude.

The dependency of the breakdown probability of free-bubble-guided UPSDs on the gas flow rate is illustrated in Fig. 2(b). The initial breakdown probability is 55% when the gas flow rate is zero, referring to untriggered UPSDs. Then, the breakdown probability starts to increase with the increase in the gas flow rate before it reaches 10 SCCM. This is due to the increased general size and elevation speed of the injected bubble providing a larger favourable low density area for electric filed enhancement for streamers' formation and propagation. However, with the further increase in gas flow rate, the breakdown probability turns to decrease. This tendency can be reasonably explained by an experimental observation that the movement of injected bubble became more violent and successive injected bubbles began to appear in between inter-electrode gap with increased gas glow rate. These phenomena caused intensive fluctuation of the bulk water which was likely to disturb the propagation of streamers. Therefore, although the injection of gas bubbles helps to improve the breakdown probability of UPSDs, the dynamics of the injected bubble should be controlled in an appropriate manner to prevent its disturbance to the development of streamers.

The pre-breakdown delay, T_d, is referred to the time used by the formation of streamers and the complete bridging of the plasma channel, i.e., the time interval between the application of the voltage impulse and the breakdown moment. Shorter pre-breakdown delay indicates less energy loss, which is beneficial to deliver more electrical energy to the plasma channel and thereby to generate stronger acoustic waves. As mentioned in previous section, the presence of the injected bubble provides a potential 'shortcut' for the streamer's propagation, therefore, its corresponding influence of the injected bubble on the pre-breakdown delay has been analyzed in this paper.

This is a peer-reviewed, accepted author manuscript of the following research article:
Guo, X., Sun, Y., Liu, C-L., Jing, L., Zhang, Y-T., Wang, X-L., & Timoshkin, I. (2022). The guiding effect of artificially injected gas bubble on the underwater pulsed spark discharge and its electrical and acoustic parameters after breakdown. Physics of Plasmas, 29(11), [113504]. https://doi.org/10.1063/5.0122080

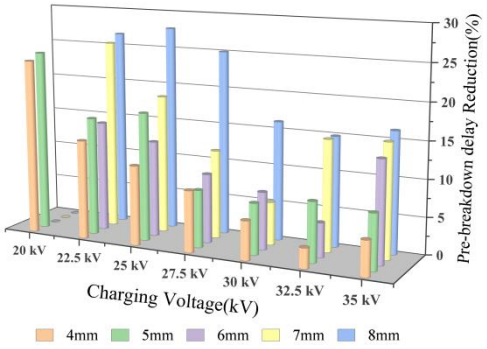

FIG.3. The pre-breakdown delay reduction of gas-bubble-guided UPSDs as compared with untriggered UPSDs under different discharge conditions.

The pre-breakdown delay reduction by injecting gas bubble in UPSDs, as compared with untriggered UPSDs, for different combination of discharge parameters is shown in Fig. 3. The delay reduction was defined as $T_{d\text{-}reduction} = (T_{d\text{-}untriggered} - T_{d\text{-}bubble})/T_{d\text{-}untriggered}$. It is worth of note that inter-electrode gap distances, including 6, 7 and 8 mm, were unable to break down by using voltage impulse with amplitude of 20 kV, in which case, values of $T_{d\text{-}reduction}$ for these circumstances were recorded as 0. It can be seen that the reduction of pre-breakdown delay introduced by the injection of bubbles in UPSDs varied from 5% to 28%. Similar to the observation that the breakdown probability is enhanced by the injected bubble as shown in Fig. 2, the delay reduction effect induced by the injection of free bubble is more significant in long gap distances under the energization of voltage impulse with relatively low amplitude, for example in 7 mm and 8 mm gaps together with 22.5 kV and 25 kV charging voltage. This observation can be explained by the fact that the random propagation nature of streamers, together with slow propagation speed due to weaker voltage impulse, in free dielectric space aggravates the potential length of plasma channel in long inter-electrode gaps. The presence of the bubble, acting as an electric field enhancement area, boosts the formation of continuing streamers and guides their forward direction to the opposite electrode. In this case, the injected bubbles play a significant role in guiding the plasma channel, disguised as shortening the propagation distance in the bulk water, increasing the breakdown probability and reducing the pre-breakdown delay, which will be studied experimentally and numerically in following sections.

2. Bubble dynamics under the influence of pulsed electric field

The electric field present in the vicinity of the injected air bubble is enhanced due to the mismatch in the permittivity of the air and the dielectric water, which is highly dependent on the shape of the bubble. The original elevation dynamics of a free bubble in stationary water is subjected to a series of physical laws, including buoyancy, gravity, surface tension and so on. The presence of the applied voltage induces additional electric stress performed on the surface of a bubble (gas-liquid surface), which causes deformation of the bubble during its development [33]. This particular deformation further influences the electric field distribution and thereby potentially alters its guiding mode in UPSDs. Therefore, it is important to clarify the deformation phenomenon of the injected bubble in water under the influence of applied voltage.

This is a peer-reviewed, accepted author manuscript of the following research article:
Guo, X., Sun, Y., Liu, C-L., Jing, L., Zhang, Y-T., Wang, X-L., & Timoshkin, I. (2022). The guiding effect of artificially injected gas bubble on the underwater pulsed spark discharge and its electrical and acoustic parameters after breakdown. Physics of Plasmas, 29(11), [113504]. https://doi.org/10.1063/5.0122080

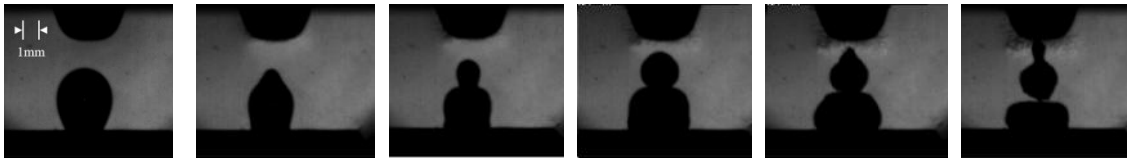

FIG.4. Shadowgraph images for the deformation of injected bubble under the influence of a applied voltage impulse with amplitude of 20 kV at 7 mm without breakdown. The fps of the camera was 50000 and the exposure time is 4 μs. The top shadow is the HV electrode and the bottom shadow is the ground electrode.

The evolution of the shape of an injected bubble under the influence of a voltage impulse without breakdown is shown in Fig.4. It can be seen that the original shape of the bubble, initiated from the ground electrode, was close to a sphere with the diameter of 3 mm. After the appearance of the pulsed electric field indicated by the fluid disturbance in the vicinity of the upper HV electrode, the deformation started from the top half of the bubble, getting elongated and becoming pointed. As time went by, the top half of the bubble tended to become an individual sphere, apart from the bottom half of the original bubble, as its middle area was squeezed tightly. Similar deformation seemed to occur again to the upper split bubble.

As mention above, this type of bubble deformation can be contributed to the electric stress, F_{elec}, performed on the gas-liquid surface. Such electric stress can be expressed as the divergence of the Maxwell stress tensor [33]:

$$\boldsymbol{F}_{elec} = \varepsilon_0 \varepsilon_r (\nabla \cdot \boldsymbol{E}) \cdot \boldsymbol{E} - \nabla \frac{\varepsilon_0 \varepsilon_r}{2} \boldsymbol{E}^2 + \nabla \frac{\rho}{2} \boldsymbol{E}^2 \frac{d\varepsilon_0 \varepsilon_r}{d\rho} \tag{1}$$

where E is the electric field, ε_0 is the vacuum dielectric constant, and ε_r is the relative dielectric constant of water; ρ is the density of the water. The value of $\varepsilon_0 = 8.854 \times 10^{-12}$ F/m, $\varepsilon_r = 78$ and $\rho = 1000$ kg/m^3 were used in this study. The first term on the right side of (1) indicates the Coulomb force due to the presence of net electric charge at the interface and the second term refers to the electrophoretic force as a result of the change in the permittivity for different dielectrics. The third term represents the electrostriction force. In this paper, we assumed that the fluid was incompressible with constant density and dielectric constant, in which case, the third term was excluded in this study. [38,39]

In order to study how the electric stress, manipulate the deformation of the injected bubble in incompressible water, a numerical study was conducted based on (1) embedded with the phase field method, which has been verified to be effective in dealing with the two-phase flow motion [40].

Fig.5 shows the numerical results obtained for deformation of an injected bubble under three different types of energization condition. Fig. 5 illustrates the structural configuration of the numerical model used to simulate the experimental setup of the free-bubble-guided UPSDs for all three cases and the bubble was initially set to be in sphere shape for modelling simplification. Fig. 5 (a) was obtained without the presence of an electric field and used as a control group. Fig. 5(b) and Fig. 5(c) was obtained by using a voltage impulse to the pointy HV electrode with the amplitude of 10 kV and 20 kV respectively, among which, Fig. 5(b) and Fig. 5(c) shows the F_{elec} developed on the gas-liquid surface at 0.0156 μs after the application of corresponding voltage impulses, which were decomposed as a vertical component and a horizontal component.

It can be seen from Fig. 5(a) that the injected bubble remained in relatively intact spherical shape in the control group. Its gas-liquid surface was only slightly deformed, following the natural dynamics of a bubble in bulk water. However, when an electric field (generated by the 10 kV voltage impulse) appeared in the inter-electrode gap, the corresponding F_{elec} was present on the gas-liquid surface of the injected bubble, as shown in Fig. 5(b). Although both of the vertical and the horizontal components of F_{elec} were pointing to the inside of the bubble, the horizontal one had dominated the vertical one for most of the time during the existence of the electric field. Therefore, the general deformation of the injected bubble tended to exhibit as elongation along vertical direction. When the amplitude of the voltage impulse was increased to 20 kV, the horizontal

This is a peer-reviewed, accepted author manuscript of the following research article:
Guo, X., Sun, Y., Liu, C-L., Jing, L., Zhang, Y-T., Wang, X-L., & Timoshkin, I. (2022). The guiding effect of artificially injected gas bubble on the underwater pulsed spark discharge and its electrical and acoustic parameters after breakdown. Physics of Plasmas, 29(11), [113504]. https://doi.org/10.1063/5.0122080

component of F_{elec} was significantly enhanced and grew much stronger than that in the case of 10 kV voltage impulse, as shown in Fig. 5(c). This result led to more intensive shrinkage initiating from the middle position of the bubble body, and the intact bubble tended to split into two individual smaller ones during its subsequent deformation period, which agrees with the experimental observation obtained for the deformation of the injected bubble shown in Fig. 4.

Similar deformation pattern was also obtained for Nitrogen gas bubble present in dielectric liquid FC-72 under the influence of a DC voltage in [41], and the dependency of the bubble's deformation degree on the amplitude of the applied voltage was also confirmed to be positive. It can be predicted that the injected bubble is likely to deform more rapidly and violently and to transform into multiple smaller bubbles with further increase in either the amplitude or the pulse width of the applied voltage impulse for the discharge geometry used in this paper.

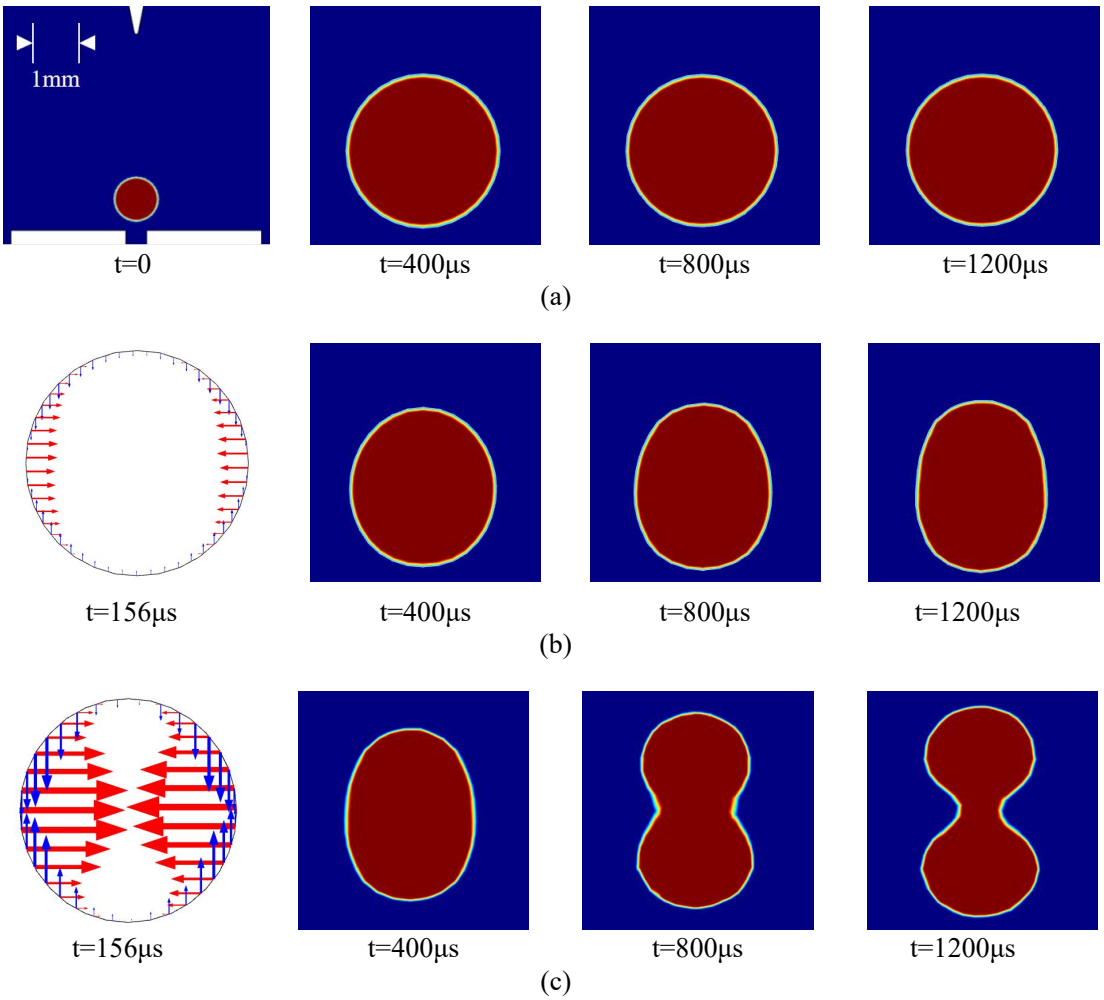

FIG.7. Numerical results obtained for the deformation of the injected bubble and F_{elec} performed on the gas-liquid surface at a specific moment under a voltage impulse (featured pulsed width of 400 μs) with amplitude of (a) 0 kV, (b) 10 kV and (c) 20 kV at 4.5 cm. The coloring scaling shows the variation of the volume fraction as the gas phase over the liquid phase, the deep blue indicating pure liquid and the deep red indicating pure gas. The gas-liquid surface refers to the value of the volume fraction at 0.5 as half gas phase and half liquid phase. The blue arrows show the vertical component of F_{elec} while the red arrows show the horizontal component of F_{elec}. The relative size of these arrows indicates the intensity of the stress.

This is a peer-reviewed, accepted author manuscript of the following research article:
Guo, X., Sun, Y., Liu, C-L., Jing, L., Zhang, Y-T., Wang, X-L., & Timoshkin, I. (2022). The guiding effect of artificially injected gas bubble on the underwater pulsed spark discharge and its electrical and acoustic parameters after breakdown. Physics of Plasmas, 29(11), [113504]. https://doi.org/10.1063/5.0122080

3. Guiding mechanism of injected bubble on pre-breakdown process

The injection of bubble is able to alter the local distribution of the applied electric field and generates a favorable area for the initiation and the development of plasma streamers for UPSDs. As compared with untriggered UPSDs, gas-bubble-guided UPSDs provide outstanding advantage in the promotion of breakdown probability and in the reduction of pre-breakdown energy loss. Such guiding effect of injected bubbles on the pre-breakdown stage of UPSDs were studied by using shadowgraph diagnostics.

Fig. 6 shows the development of a UPSD in untriggered mode. It can be found that two plasma streamers were initiated from the head of the HV electrode and transformed into branching patterns. These streamers propagated in a random manner, only one of which dominated in developing process and became the first to contact the opposite ground electrode, forming a complete plasma channel and achieving the breakdown.

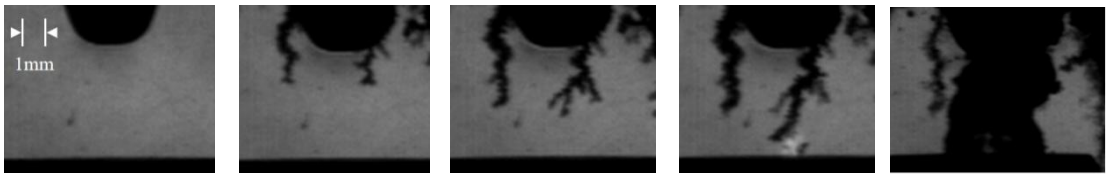

FIG. 6. Shadowgraph images for development process of free breakdown flow injection in water. The amplitude of the applied voltage impulse was 25 kV. The fps of the camera was 40000 and the exposure time is 4 μs.

The development process of the pre-breakdown stage with the presence of the injected bubble is shown in Fig. 7. The injected bubble was initially located on the bottom of the ground electrode. Similar to the case of untriggered UPSDs, multiple plasma streamers were formed at the HV electrode after the immediate appearance of the voltage impulse and started to propagate to the ground electrode in a branching pattern as well. Meanwhile, the injected bubble started to follow the similar deformation tendency demonstrated in Fig. 4. Then, one of the generated streamers, the second one from left at 200 μs in Fig. 7, contacted the bubble from its left side and thereby electrically connected to the ground electrode. Finally, the primary plasma channel was formed along this particular streamer's propagation pathway and the breakdown strike occurred. It is worth of note that the streamer leading to the breakdown in this case was not the longest one. The injected bubble electrically shortened the distance between the effective streamer and the ground electrode. This observation verifies the guiding effect of the injected bubble on the streamers' development process for UPSDs.

FIG. 7. Shadowgraph images for guided image of the free bubble on the discharge. The amplitude of the applied voltage impulse was 25 kV. The fps of the camera was 40000 and the exposure time is 4 μs. The top is the high voltage electrode shadow, the middle is the bubble shadow, and the bottom is the ground electrode.

To figure out the influence of the relative position of the injected bubble on its guiding effect, the fixed-bubble electrode set was used to achieve UPSDs. By alternating the experimental arrangement of the capillary tube, the position of the fixed-bubble was accordingly adjusted.

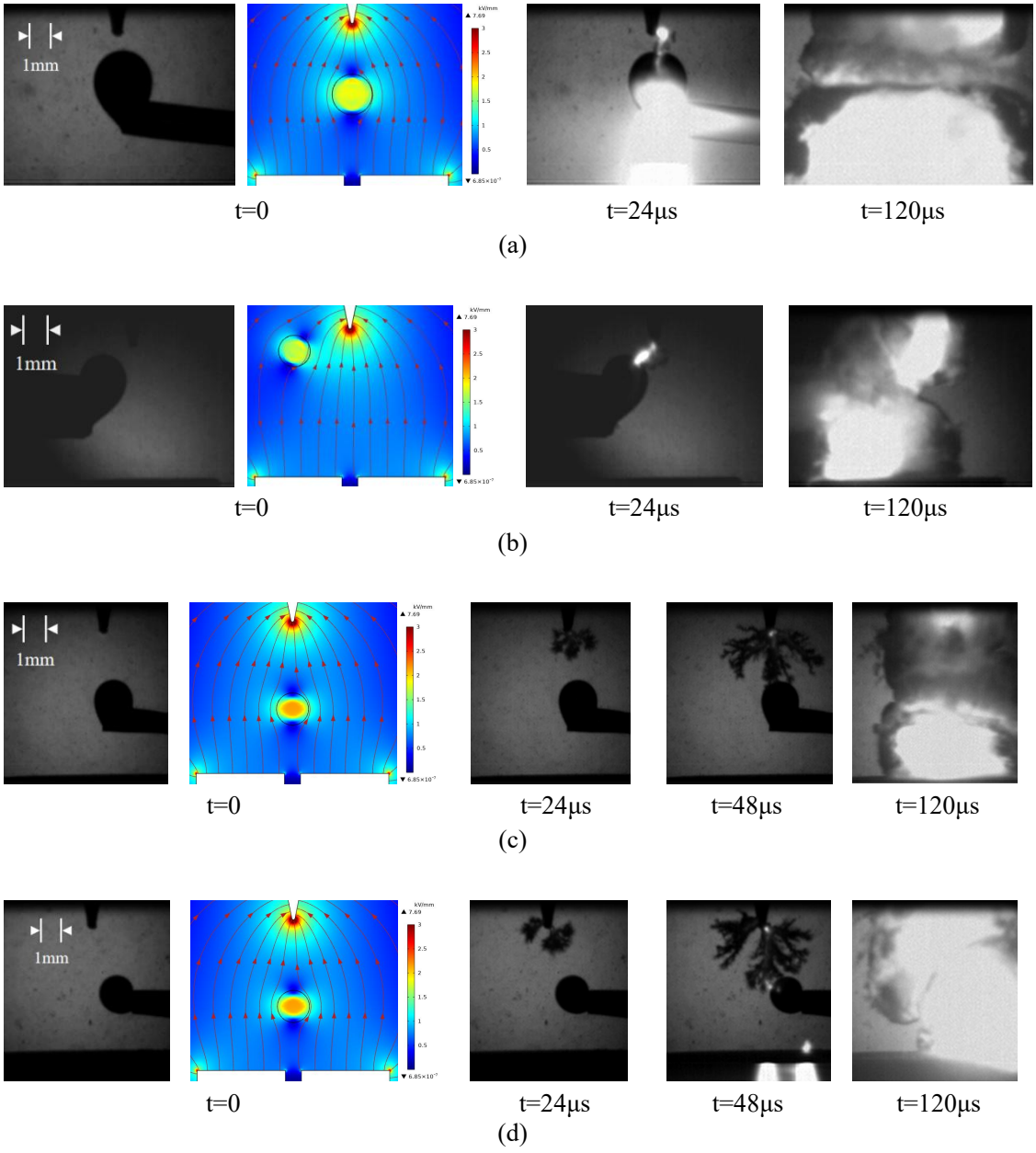

FIG.8. Shadowgraph images for the pre-breakdown process of gas-bubble-guided UPSDs and their calculated initial electric field distribution (expressed in kV/mm), using a voltage impulse of 20 kV, for different bubble positions as (a) centrally close to HV electrode, (b) a distance horizontally displaced from central close to HV electrode, (c) centrally away from HV electrode and (d) a distance horizontally displaced from central away from HV electrode. The fps of the camera was 40000 and the exposure time is 4 μs. The color scaling of the calculated results indicates the intensity of the electric field, where cold colors represent lower electric field strength and warm colors represent higher electric field strength.

Fig. 8(a)-(d) show the guiding mechanism of the fixed-bubble with different position arrangements, together with the initial electric field distribution obtained at the appearance moment of the voltage impulse. It can be found that the primary streamer made contact with the fixed-bubble at first and the subsequent bridging between the bubble and the ground electrode was completed rapidly for all four bubble's position arrangements (even when the bubble was located

horizontally biased from the central position of the electrode geometry, as indicated in Fig. 8(b) and Fig. 8(d), since the local electric field strength in vicinity of the bubble was intensified, especially at its left and right sides.

A distinct observation is that only an individual primary streamer was formed directly connecting the HV electrode tip and the bubble surface when the bubble was spatially close to the HV electrode, as shown in Fig. 8(a) and Fig. 8(c), and the generated streamers produced strong light emission, potentially indicating large amount of charge injection. When the bubble was located away from the HV electrode in the cases of UPSDs shown in Fig. 8(b) and Fig. 8(c), multiple branches of streamers were initiated and developed along the electric field lines. Once one of these streamers got in touch with the bubble, it turned into the primary streamer and generated light emission, which was weaker than that observed in Fig. 8(a) and Fig. 8(b), though the enhancement of the electric field inside the bubble in the two cases seemed to be more significant. Therefore, it can be deduced that when the bubble is present close to the HV electrode stronger primary streamer is likely to be generated and thereby results in faster breakdown process and larger amount of electrical energy potentially delivered into the plasma channel.

It is worth of note that there was lack of convincing experimental evidence indicating whether the streamer's development was inside the bubble or along the gas-liquid surface in the present work. As reported in [16, 31], streamers seemed to be initiated and propagated inside the bubble when it was originally in direct contact the HV electrode. In [32], it was pointed out streamers were likely to travel along the bubble surface when the bubble was distant from the HV electrode.

B. Electrical and acoustic parameters after breakdown

After the occurrence of breakdown, intensive inductive current injects large amount of electrical energy, stored originally in the capacitance, into the pulsed power circuit. Due to the resistance existed in the circuit and in the plasma channel, the majority of the stored energy is consumed by these two resistive components and such energy dissipation rules can be described by the electrical parameters, including the breakdown voltage, the circuit resistance, the plasma resistance, the plasma energy and the plasma energy density. The acoustic performance of gas-bubble-guided UPSDs can be evaluated by using the acoustic parameters, including the acoustic amplitude and the acoustic efficiency. These parameters were derived from the voltage, current and acoustic signals recorded during experiments. Their relationships help to analyze the energy distribution mechanism and to conclude how desirable UPSDs can be achieved for better acoustic emission with satisfactory energy efficiency.

The typical plasma-acoustic signals of a gas-bubble-guided UPSD are shown in Fig 9. The negative voltage impulse reached its maximal value rapidly with the closure of the spark switch. After a specific delay, the breakdown event occurs and the breakdown voltage V_{br}, referred to the value of the voltage at the breakdown moment when significant oscillation started to appear in both voltage and current waveforms. Such oscillations corresponded to the presence of the RLC elements in the pulsed power circuit after breakdown, shown as the simplified equivalent circuit in Fig. 10. C represents the energy storage capacitance and L_{cir} is the inherent inductance of the circuit (mainly contributed by the switching spark), R_{cir} is the intrinsic resistance of the circuit, potentially existing in, for example, the capacitors, the switching gap and the HV transmission lines. The value of R_{pl} and L_{pl} represent the resistance and inductance of the plasma channel respectively.

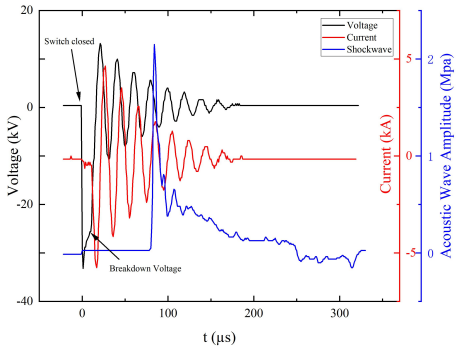

FIG. 9. Typical voltage and current waveforms, and first impulse of acoustic wave obtained for a gas-bubble-guided UPSD in a 5 mm gap with breakdown voltage of 25 kV. The position of the hydrophone was 20 cm away from the spark source.

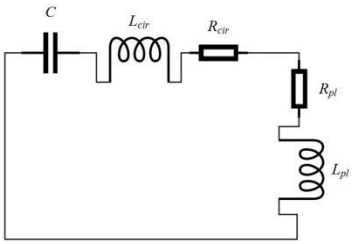

FIG.10. Simplified discharge circuit.

In this case, the electrical parameters of the gas-bubble-guided UPSDs can be determined by using underdamped second order circuit solutions [17, 19, 32]:

$$i(t) = I_0 e^{-\alpha t} \sin(\omega t) \tag{2}$$

$$R = 2L\alpha \tag{3}$$

$$I_0 = V_{br} C \left(\frac{\alpha^2}{\omega} + \omega \right) \tag{4}$$

$$\omega_0^{\,2} = \omega^2 + \alpha^2 = \frac{1}{LC} \tag{5}$$

where R is the total resistance present in the circuit as R_{cir}+R_{pl} and the R_{cir} was calculated to be 0.572 Ω when the gap is short circuited. L is the total inductance of the circuit, containing L_{cir} and L_{pl} components, which differs for different breakdown voltages.

Then, the electrical energy deposited in the plasma channel is:

$$E_{pl} = R_{pl} \int i(t)^2 dt \tag{6}$$

The acoustic signal was captured after a specific time delay, as shown in Fig. 9, due to the horizontal distance between the hydrophone and the spark source. The acoustic amplitude was represented by the pressure value of the first peak in the waveform and the energy stored in an acoustic impulse, E_{ac}, is given by:

$$E_{ac} = \frac{4\pi d^2}{\rho_\infty c_\infty} \int P_{ac}(t)\, dt \tag{7}$$

where P_{ac} is the acoustic waveform, ρ_∞ is the density of the water, 1000 kg/m^3, c_∞ is the local propagation speed of a pressure wave as 1500 m/s, d is the distance between the hydrophone and the spark source, which was 20 cm in this paper. It should be point out that only the first impulse of the acoustic signal was used for analysis conducted in this paper.

Therefore, the acoustic energy conversion efficiency is defined as:

$$\eta_{ac} = \frac{E_{ac}}{E_{pl}} \tag{8}$$

1. Fundamental electrical parameters: plasma resistance and plasma energy

As seen in Fig. 11, the energy distribution in between the plasma channel and the external circuit relays on the relationship between their resistance. According to the RW model [37], the resistance of a plasma channel is a function of the inductive current after breakdown, in which case, the dependency of the plasma resistance, R_{pl}, and its relationship with the circuit resistance, R_{cir}, on the breakdown property, V_{br}, play important roles in determining the plasma energy, E_{pl}.

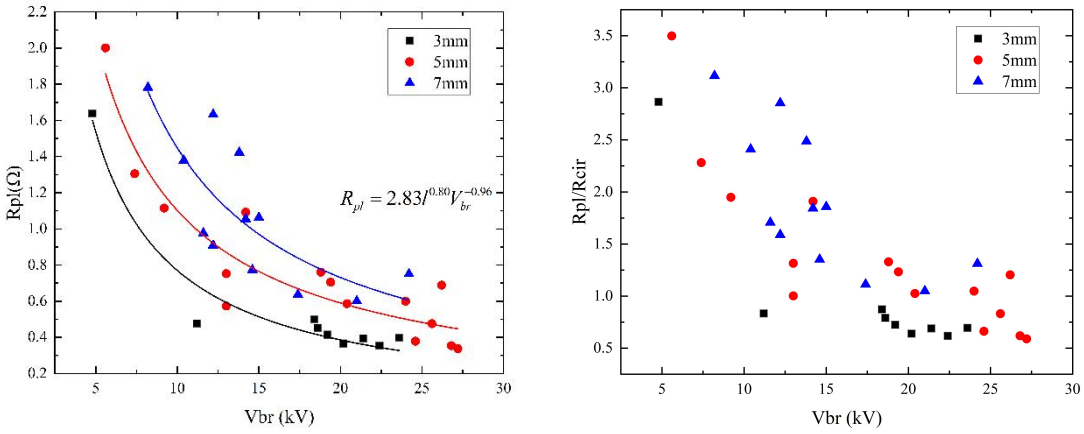

FIG. 11. The dependency of (a) R_{pl} and (b) ratio between R_{pl} and R_{cir} on V_{br} for three different gap distances. The black, red and blue lines correspond to the fitting results of (9) for 3 mm, 5mm and 7mm respectively and their fitting correlation coefficients are 0.96, 0.87, 0.63 accordingly.

The dependency of R_{pl} and the ratio between R_{pl} and R_{cir} on the the along with the breakdown voltage for three different gap distances, l, including 3 mm, 5 mm and 7 mm, is shown in Fig. 11(b).

It can be seen from Fig. 11(a) that the value of R_{pl} decreases with the increase in the breakdown voltage for all three gap distance cases. Larger values of V_{br} lead to larger discharge current, so that the conductivity of the plasma channel is higher, resulting in the significant reduction in R_{pl} for larger V_{br}. It is also clear from Fig. 11(a) that, for same value of V_{br}, R_{pl} has higher value for longer l, as the resistance was in proportion to the length of the resistive plasma channel. Thus, a phenomenological R_{pl} is given as:

This is a peer-reviewed, accepted author manuscript of the following research article:
Guo, X., Sun, Y., Liu, C-L., Jing, L., Zhang, Y-T., Wang, X-L., & Timoshkin, I. (2022). The guiding effect of artificially injected gas bubble on the underwater pulsed spark discharge and its electrical and acoustic parameters after breakdown. Physics of Plasmas, 29(11), [113504]. https://doi.org/10.1063/5.0122080

$$R_{pl} \propto x l^{n} V_{br}^{\beta} \tag{9}$$

where x is a proportionality coefficient, n and β are the power coefficients for l and V_{br} (expressed in mm and kV) respectively.

By applying experimental data into (9), the numerical values of x, n and β could be obtained. The fitting effect of (9) is demonstrated by the colored lines in Fig. 11(a) for different gap distances and its agreement with the experimental data was satisfactory. Therefore, the final form of the relation for R_{pl} is given as:

$$R_{pl} = 2.83 l^{0.80} V_{br}^{-0.96} \tag{10}$$

By introducing the constant R_{cir}, Fig. 11(b) shows the variation of the resistance ratio between the plasma channel and the external circuit, R_{pl}/R_{cir}, in percentage as a function of V_{br}. The variation tendency is similar to the relationship between R_{pl} and V_{br} as shown in Fig. 11(a). The reduction in R_{pl}/R_{cir} indicates that less amount of available energy at breakdown was to be delivered into the plasma channel and the most of which would be dissipated into the circuit. This trend is more significant when V_{br} is large at a short gap distance.

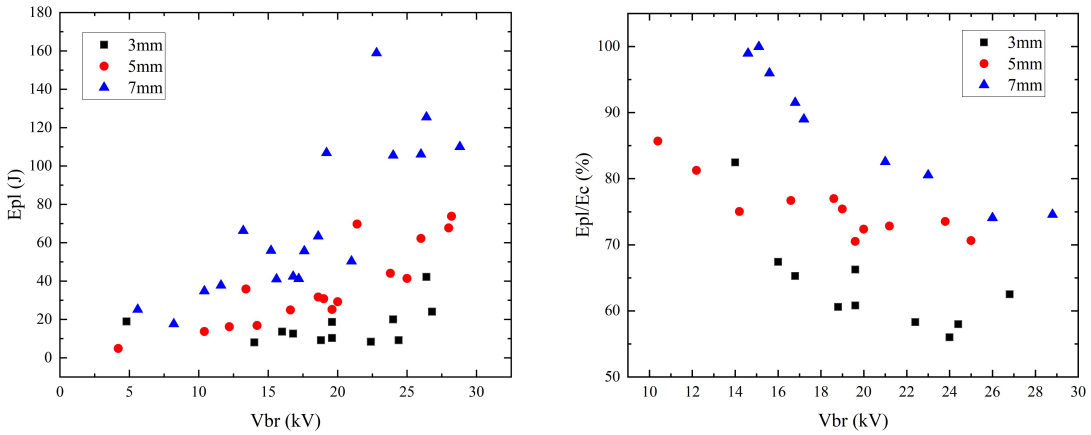

FIG. 12. The dependency of (a) E_{pl} and (b) the energy conversion proportion on V_{br} for three different gap distances.

The plasma energy, E_{pl}, was obtained using (6). and the energy conversion proportion from capacitors to plasma, was defined as the ratio between E_{pl} and the electrical energy stored in capacitors at breakdown moment, E_c, where E_c was calculated by $E_c = CV_{br}^2/2$, was regarded as energy conversion efficiency from the storage capacitors to the plasma. The relationships between E_{pl}, E_{pl}/E_c and V_{br} for for three gap distances are shown in Fig.12. It is found that larger values of E_{pl} and E_{pl}/E_c were always obtained in long gap distance. Different from R_{pl}, E_{pl} has demonstrated an increasing trend with the increase in V_{br} though the value of E_{pl}/E_c is becoming lower and lower. This observation reveals a fact that it is a feasible method to increase the plasma energy by elevating the breakdown voltage level, thereby the acoustic emission could be enhanced accordingly as reported in[19]. However, a sacrifice has to be made by using this approach for the promotion of E_{pl} that more electrical energy will be wasted in R_{cir} as higher E_{pl} brings lower energy conversion proportion from E_c to E_{pl}, and then less electrical energy works in improving E_{pl}.

This is a peer-reviewed, accepted author manuscript of the following research article:
Guo, X., Sun, Y., Liu, C-L., Jing, L., Zhang, Y-T., Wang, X-L., & Timoshkin, I. (2022). The guiding effect of artificially injected gas bubble on the underwater pulsed spark discharge and its electrical and acoustic parameters after breakdown. Physics of Plasmas, 29(11), [113504]. https://doi.org/10.1063/5.0122080

2. Dependency of plasma energy density on breakdown voltage

Different from untriggered UPSDs, the injected bubble is able to regulate streamers' propagation, as discussed in Section A, and helps to form relatively straight plasma channel with the length of which is approximately equal to the gap distance, stabilizing the breakdown performance of UPSDs. It is possible to take a deeper look inside the plasma energy density, defined as the plasma energy per unit length, $D_{pl} = E_{pl}/l$. Its relationship with the electrical parameter, V_{br}, helps to understand the characteristics of the plasma energy dissipation under different discharge conditions.

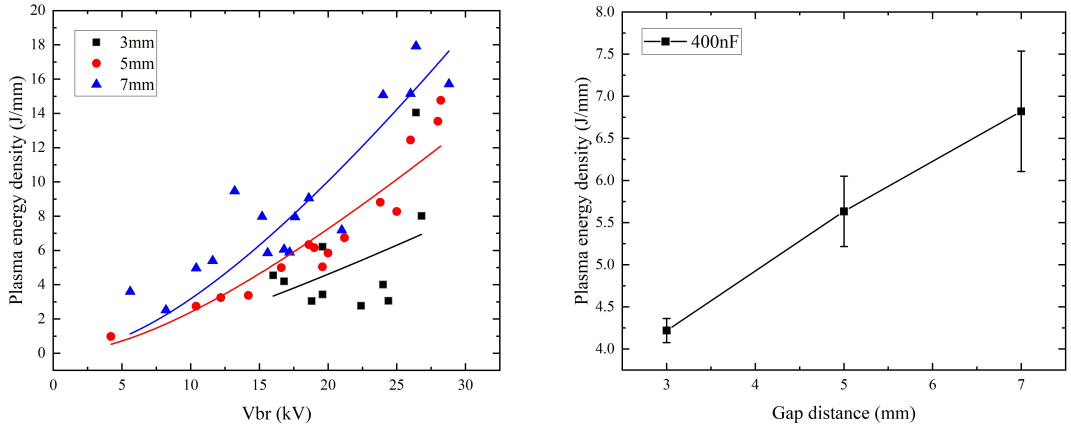

FIG. 13 (a) The variation of the plasma energy density as a function of the breakdown voltage for three different gap distances, (b) the relationship between the plasma energy density and the gap distance, obtained for UPSDs with V_{br} varying from 18 kV to 20 kV. The black, red and blue lines correspond to the fitting of (15) for 3 mm, 5 mm, and 7 mm, their fitting correlation coefficients are 0.81, 0.89, 0.67 respectively.

Fig. 13 shows the functional behavior of the plasma energy density for three different gap distances and the dependency of its average values on the gap distance. It can be seen from Fig. 13(a) that D_{pl} shows an increasing trend with the increase in V_{br} and is larger in longer gaps. The increase in V_{br} brings in larger amount of electrical energy to be delivered in the plasma channel. By assuming that the plasma energy is evenly distributed along the channel, the resultant plasma energy density would grow with the increase in V_{br}. It is also clear in Fig. 13(b) that the value of D_{pl} is higher in longer gaps for similar values of V_{br}. As seen in Fig. 13(b), the value of R_{pl} for longer gaps is generally larger than that for shorter gaps, meaning more electrical energy to be dissipated in longer plasma channel when considering same amount of electrical energy available at breakdown. This type of enhancement of the plasma energy dominates the influence of the plasma channel's extension, resulting in continuing increase in D_{pl} for gas-bubble-guided UPSDs achieved in long gaps.

The tendency shown in Fig. 11(a) can be described by a relation established using (10) and the electrical energy distribution relationship between R_{pl} and R_{cir}. Such a relation can be derived as following:

$$\frac{E_{pl}}{E_{pl}+E_{cir}} = \frac{R_{pl}}{R_{pl}+R_{cir}} \tag{11}$$

$$E_{pl}+E_{cir} \propto E_C \tag{12}$$

$$E_C = \frac{1}{2}CV_{br}^2 \tag{13}$$

This is a peer-reviewed, accepted author manuscript of the following research article:
Guo, X., Sun, Y., Liu, C-L., Jing, L., Zhang, Y-T., Wang, X-L., & Timoshkin, I. (2022). The guiding effect of artificially injected gas bubble on the underwater pulsed spark discharge and its electrical and acoustic parameters after breakdown. Physics of Plasmas, 29(11), [113504]. https://doi.org/10.1063/5.0122080

$$E_{pl} \propto \frac{R_{pl}}{R_{pl}+R_{cir}} E_C \tag{14}$$

By substituting R_{pl} and E_c with (11) and (14), (15) can be rewritten as:

$$D_{pl} = \frac{E_{pl}}{l} = A\frac{CV_{br}^2}{2l}\frac{1}{1+R_{cir}/(2.83l^{0.8}V_{br}^{-0.96})} \tag{15}$$

where $A = xl^n$, as D_{pl} is also a function of l as seen in Fig. 13(b), x is a proportionality coefficient.

By fitting (15) to experimental data in Fig. 13(a), the phenomenological expression for D_{pl} can be obtained as:

$$D_{pl} = \frac{E_{pl}}{l} = k\frac{CV_{br}^2 l^{0.49}}{1+R_{cir}/(2.83l^{0.8}V_{br}^{-0.96})} \tag{16}$$

where $k = 4.2\times10^{-5}$.

The results of (16), demonstrated as the colored line in Fig. 13 (a), have shown reasonable agreement with the experimental data, especially for 5 mm and 7 mm cases, while there is lack of effective data points for better fitting effect in 3 mm case.

3. Acoustic parameters: acoustic wave amplitude and acoustic efficiency

As reported in [19], the amplitude of the UPSD-generated AW is proportional to V_{br}. With the knowledge of the increment in V_{br} promoting D_{pl}, the positive correlation between the acoustic parameter and D_{pl} can be expected. Fig. 14 shows the relationship between the acoustic wave amplitude and the plasma energy and also the variation of the acoustic efficiency, η_{ac}, as a function of the breakdown voltage.

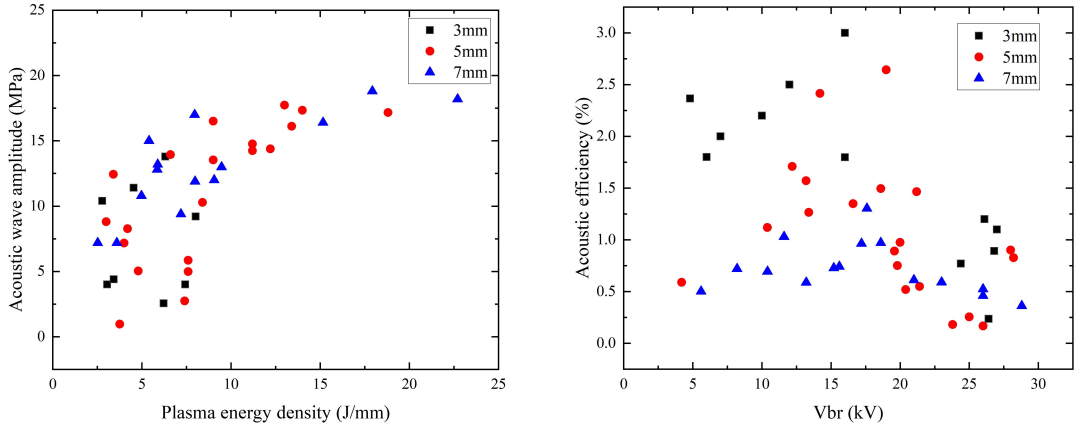

FIG. 14. (a) Dependency of the acoustic wave amplitude on the plasma energy density at different discharge gaps, (b) variation of acoustic efficiency as a function of V_{br} for different gap distances.

It can be seen from Fig. 14(a) that the amplitude of the acoustic wave shows a non-linear increasing trend with the increase in the plasma energy density. For lower values of D_{pl}, ranging from 2 J/mm to 10 J/mm, the acoustic wave amplitude increases rapidly while it slows down for D_{pl} larger than 10 J/mm, meaning there might being a potential upper limitation of D_{pl} where the acoustic wave amplitude sees not more significant improvement. For the purpose of continuing increase in the acoustic wave amplitude, the electrical energy injection rate (electrical power) should be a primary factor to manipulate, especially in the initial stage of the discharge current [17]. Fig. 14(b) shows that η_{ac} initially increases following the increase in V_{br} and discharges in longer gap achieve better η_{ac} for same value of V_{br}. However, η_{ac} starts to decrease when V_{br} increases larger than approximately 17.5 kV. This variation of η_{ac} can be explained as that the acoustic energy, E_{ac}, increases faster than the increase in D_{pl} before D_{pl} reaches a special point at 10 J/mm, corresponding to V_{br} of 17.5 kV, when still resulting in the increase in η_{ac}. Beyond this specific point, the increment in E_{ac} slows down, as indicated in Fig. 14(a), and cannot follow the increment in D_{pl}, in which case, the resultant η_{ac} turns to decrease, while the acoustic wave amplitude still tends to grow. It is concluded that although the strength of the acoustic wave can be enhanced by increasing either the breakdown voltage or together with the gap distance, the optimization of the acoustic efficiency appears to be achieved only by using appropriate voltage amplitudes, depending on the specific discharge geometry.

IV. CONCLUSION

As compared with untriggered UPSDs, the injected bubble works as an effective mechanism to facilitate the formation of streamers and to guide their propagation for promoting the electrical energy injection in the plasma channel for better acoustic performance of UPSDs. In this paper, the general influence of the bubble injection on UPSDs was evaluated by the breakdown probability and pre-breakdown delay. Both experimental and numerical studies were conducted to investigate the dynamics of the injected bubble under the influence of a voltage impulse and to clarify the guiding modes of the injected bubble in UPSDs. The electrical energy distribution relationship between the plasma and the external circuit was studied by analyzing the relationships between electrical parameters, including the breakdown voltage, the plasma resistance, the plasma energy and the plasma energy density. The acoustic wave amplitude and the acoustic efficiency were also obtained as a function of these electrical parameters.

The injection of bubble in between inter-electrodes gap brought significant improvement in the breakdown probability and also in the pre-breakdown delay reduction, especially when achieving UPSDs in relatively long gap distance with low voltage level. Also, there was an optimal choice of the gas flow rate as too high the bubble injection speed would disturb the stationary bulk water violently and interfere the discharge process.

It was found that the injected bubble would deform as a result of the electric stress performed on the gas-liquid surface. Such deformation degree depended on the amplitude of the voltage impulse. Higher voltage induced stronger horizontal component of the electric stress, developed somewhere near the middle part of the bubble body, and the subsequently squeezed bubble tended to transformed into multiple smaller ones.

During the pre-breakdown process of the gas-bubble-guided UPSDs, a primary streamer was formed connecting the HV electrode and the injected bubble. Then, a complete plasma channel was established between the bubble and the ground electrode. A branch of bright plasma streamer was more likely to appear when the bubble was spatially close to the HV electrode.

The plasma resistance would decrease with the increase in the breakdown voltage. Although the energy conversion efficiency from E_c to E_{pl} decreased correspondingly, the absolute amount of E_{pl} still kept an increasing trend as well as the plasma energy density, D_{pl}. Phenomenological scaling relations, (10) and (15), were used to describe the dependency of R_{pl} and D_{pl} on V_{pl}.

The amplitude of the acoustic wave initially increased rapidly as higher plasma energy density was achieved using higher breakdown voltage, and so does the acoustic efficiency. When the breakdown voltage went higher than a specific point (as 17.5 kV in present work), the acoustic efficiency started to reduce as the acoustic wave amplitude did not change significantly.

These results will provide solid support for understanding the pre-breakdown mechanism of gas-bubble-guided UPSDs and help to distinguish the importance of different injected bubbles'

This is a peer-reviewed, accepted author manuscript of the following research article:
Guo, X., Sun, Y., Liu, C-L., Jing, L., Zhang, Y-T., Wang, X-L., & Timoshkin, I. (2022). The guiding effect of artificially injected gas bubble on the underwater pulsed spark discharge and its electrical and acoustic parameters after breakdown. Physics of Plasmas, 29(11), [113504]. https://doi.org/10.1063/5.0122080

properties in manipulating the breakdown process. The obtained relationships can be used in pursuing ideal acoustic parameters of the plasma-acoustic system for specific practical applications.

ACKNOWLEDGEMENTS

This work was supported by National Natural Science Foundation of China (Nos. 51907108).

Data Availability Statement: The data that support the findings of this study are available from the corresponding author upon reasonable request.

REFERENCES

[1] Y. Krasik, A. Fedotov, D. Sheftman, S. Efimov, A. Sayapin, V. Gurovich, D. Veksler, G. Bazalitski, S. Gleizer and A. Grinenko. "Underwater electrical wire explosion." Plasma Sources Science and Technology 19.3 (2010): 034020.

[2] W. Hao, Z. Xi, S. Yuan and J. Liu. "Experimental and numerical investigation of ship structure subjected to close-in underwater shock wave and following gas bubble pulse." Marine Structures 39 (2014): 90-117.

[3] Y. Zhou, F. Cocks, G. Premingerm and P. Zhong. "The effect of treatment strategy on stone comminution efficiency in shock wave lithotripsy." The Journal of urology 172.1 (2004): 349-354.

[4] S. Zhu, F. Cocks, G. Preminger and P. Zhong. "The role of stress waves and cavitation in stone comminution in shock wave lithotripsy." Ultrasound in medicine & biology 28.5 (2002): 661-671.

[5] Q. Yu, H. Zhang, R. Yang, Z. Cai and K. Liu. "Experimental and numerical study on the effect of electrohydraulic shock wave on concrete fracturing." Journal of Petroleum Science and Engineering (2022): 110685.

[6] M. Wilson, L. Balmer, M. Given, S. Macgregor and I. Timoshkin. "An investigation of spark discharge parameters for material processing with high power ultrasound." Minerals Engineering 20.12 (2007): 1159-1169.

[7] W. Rutgers and I. Jong. "Multi-tip sparker for the generation of acoustic pulses." Sensor Review (2003).

[8] Y Huang, L Zhang, X Zhang, S Li, Z Liu and K Yan. "Electroacoustic process study of plasma sparker under different water depth." IEEE Journal of Oceanic Engineering 40.4 (2015): 947-956.

[9] L. Zhang, X. Zhu, Y. Huang, Z. Liu and K. Yan. "Effects of water pressure on plasma sparker's acoustic characteristics." International Journal of Plasma Environmental Science and Technology 11 (2017): 60-63.

[10] X. Wang, N. Li, J. Du and W. Wang. "Concrete crushing based on the high-voltage pulse discharge technology." Journal of Building Engineering 41 (2021): 102366.

[11] S. Inoue, S. Iizasa, D. Wang, T. Namihira, M. Shigeishi, M. Ohtsu and H. Akiyama. "Concrete recycling by pulsed power discharge inside concrete." International Journal of Plasma Environmental Science & Technology 6.2 (2012): 183-188.

[12] S. Narahara, T. Namihira, K. Nakashima, S. Inoue and H. Akiyama. "Evaluation of concrete made from recycled coarse aggregates by pulsed power discharge." 2007 16th IEEE International Pulsed Power Conference. Vol. 1. IEEE, 2008.

[13] Y. Xin, B. Sun, X. Zhu, Z. Yan, X. Zhao and X. Sun. "Resourceful treatment of alcohol distillery wastewater by pulsed discharge." Bioresource Technology 244 (2017): 175-181.

[14] L. Torres, O. Yadav and E. Khan. "A review on risk assessment techniques for hydraulic fracturing water and produced water management implemented in onshore unconventional oil and gas production." Science of the Total Environment 539 (2016): 478-493.

[15] Y. Liu, Z. Li, X. Li, S. Liu, G. Zhou and F. Lin. "Intensity improvement of shock waves induced by liquid electrical discharges." Physics of Plasmas 24.4 (2017): 043510.

[16] Q. Liu and Y. Zhang. "Shock wave generated by high-energy electric spark discharge." Journal of Applied Physics 116.15 (2014): 153302.

[17] S. Liu, Y. Liu, Y. Ren, F. Lin, H. Li and Y. Zhao. "Analysis of shock wave induced by underwater pulsed discharge using discharge current interception." Journal of Applied Physics 127.14 (2020): 143301.

[18] X. Li, Y. Liu, S. Liu, Z. Li, G. Zhou, H. Li, F. Lin and Y. Pan. "Influence of deposited energy on shock wave induced by underwater pulsed current discharge." Physics of Plasmas 23.10 (2016): 103104.

[19] Y. Sun, I. Timoshkin, M. Given, M Wilson, T. Wang, S. MacGregor, and N. Bonifaci. "Impulsive discharges in water: acoustic and hydrodynamic parameters." IEEE Transactions on Plasma Science 44.10 (2016): 2156-2166.

[20] M. Hogg, I. Timoshkin, M. Given, M. Wilson, S. Macgregor, T. Wang, R. Fouracre and J. Lehr. "Impulse breakdown of water with different conductivities." IEEE Transactions on Dielectrics and Electrical Insulation 19.5 (2012): 1559-1568.

[21] Y. Sun, I. Timoshkin, S. Macgregor, M. Wilson, M. Given, T. Wang and N. Bonifaci. "Electrical and acoustic parameters of wire-guided discharges in water: experimental determination and phenomenological scaling." IEEE Transactions on Plasma Science 45.10 (2017): 2648-2655.

[22] H. Zeghioud, P. Nguyen-Tri, L. Khezami, A. Amrane and A. Assadi. "Review on discharge Plasma for water treatment: mechanism, reactor geometries, active species and combined processes." Journal of Water Process Engineering 38 (2020): 101664.

[23] O. Higa, R. Matsubara, K. Higa, Y. Miyafuji, T. Gushi, Y. Omine, K. Naha, K. Shimojima, H. Fukuoka and H. Maehara, et al. "Mechanism of the shock wave generation and energy efficiency by underwater discharge." The International Journal of Multiphysics 6.2 (2012): 89-98.

[24] Y. Liu, Z. Li, X. Li, G. Zhou, H. Li, Q. Zhang and F. Lin. "Energy transfer efficiency improvement of liquid pulsed current discharge by plasma channel length regulation method." IEEE Transactions on Plasma Science 45.12 (2017): 3231-3239.

[25] I. Marinov, S. Starikovskaia and A. Rousseau. "Dynamics of plasma evolution in a

nanosecond underwater discharge." Journal of Physics D: Applied Physics 47.22 (2014): 224017.

[26] Y. Hayashi, N. Takada, H. Kanda and M. Goto. "Effect of fine bubbles on electric discharge in water." Plasma Sources Science and Technology 24.5 (2015): 055023.

[27] Y. Tu, Y. Xian, Y. Yang, X. Lu and Y. Pan. "Time-resolved imaging of electrical discharge development in multiple bubbles immersed in water." Plasma Processes and Polymers 14.10 (2017): 1600259.

[28] H. Fujita, S. Kanazawa, K. Ohtani, A. Komiya, T. Kaneko and T. Sato. "Initiation process and propagation mechanism of positive streamer discharge in water." Journal of Applied Physics 116.21 (2014): 213301.

[29] X. Li, Y. Liu, S. Liu, Z. Li, G. Zhou, H. Li, F. Lin, and Y. Pan. "Influence of deposited energy on shock wave induced by underwater pulsed current discharge." Physics of Plasmas 23.10 (2016): 103104.

[30] Y. Tu, H. Xia, Y. Yang, and X. Lu. "Time-resolved imaging of electrical discharge development in underwater bubbles." Physics of Plasmas 23.1 (2016): 013507.

[31] K. Tachibana, Y. Takekata, Y. Mizumoto, H. Motomura and M. Jinno. "Analysis of a pulsed discharge within single bubbles in water under synchronized conditions." Plasma Sources Science and Technology 20.3 (2011): 034005.

[32] B. Sommers and J. Foster. "Plasma formation in underwater gas bubbles." Plasma Sources Science and Technology 23.1 (2014): 015020.

[33] F. Chen, Y. Peng, Y. Song and M. Chen. "EHD behavior of nitrogen bubbles in DC electric fields." Experimental Thermal and Fluid Science 32.1 (2007): 174-181.

[34] M. Zaghdoudi and M. Lallemand. "Study of the behaviour of a bubble in an electric field: steady shape and local fluid motion." International Journal of Thermal Sciences 39.1 (2000): 39-52.

[35] P. Yang, R. Barnes, J. Mostaghimi and M. Boulos. "Application of a two-dimensional model in the simulation of an analytical inductively coupled plasma discharge." Spectrochimica Acta Part B: Atomic Spectroscopy 44.7 (1989): 657-666.

[36] J. Prados and F. Peebles. "Two-dimensional laminar-flow analysis, utilizing a doubly refracting liquid." AIChE Journal 5.2 (1959): 225-234.

[37] M. Given, I. Timoshkin, M. Wilson and S. Macgregor. "Analysis of the current waveforms observed in underwater spark discharges." 2007 16th IEEE International Pulsed Power Conference. Vol. 1. IEEE, 2007.

[38] S. Lee and I. Kang. "Three-dimensional analysis of the steady-state shape and small-amplitude oscillation of a bubble in uniform and non-uniform electric fields." Journal of Fluid Mechanics 384 (1999): 59-91.

[39] W. Dong, R. Li, H. Yu and Y. Yan. "An investigation of behaviours of a single bubble in a uniform electric field." Experimental Thermal and Fluid Science 30.6 (2006): 579-586.

[40] Q. Yang, B. Li, J. Shao and Y. Ding. "A phase field numerical study of 3D bubble rising in viscous fluids under an electric field." International Journal of Heat and Mass Transfer 78 (2014): 820-829.

[41] P. Marco, A. Faini, W. Grassi and G. Memoli. "Electric field effects on bubbles of nitrogen in FC-72 originating from a flat plate." 3rd International Symposium on Two-Phase Modelling and Experimentation, Pisa, Italy. Vol. 17. 2004.